Low Complexity Iris Recognition using Curvelet Transform

Afsana Ahamed
Department of EEE
Bangladesh University of Engineering and Technology
Dhaka, Bangladesh
afsana4@gmail.com

Mohammed Imamul Hassan Bhuiyan
Associate Professor, Department of EEE
Bangladesh University of Engineering and Technology
Dhaka, Bangladesh
imamhas@gmail.com

***Abstract*—In this paper, a low complexity technique is proposed for iris recognition in the curvelet transform domain. The proposed method does not require the detection of outer boundary and decreases unwanted artefacts such as the eyelid and eyelash. Thus, the time required for preprocessing of an iris image is significantly reduced. The zero-crossings of the transform coefficients are used to generate the iris codes. Since only the coefficients from approximation subbands are used, it reduces the length of the code. The iris codes are matched employing the correlation coefficient. Extensive experiments are carried out using a number of standard databases such as CASIA- V3, UBIRIS.v1 and UPOL. The results reveal that the proposed method using the curvelet transform provides a very high degree of accuracy (about 100%) over a wide range of images with a low equal error rate (EER) and a significant reduction in the computational time, as compared to those of the state-of-the-art techniques.**

Keywords-iris recognition; curvelet transform; correct recognition rate; equal error rate

I. INTRODUCTION

Biometric recognition systems are becoming popular in recent times due to their robustness to external effects and for the ability to offer a high degree of uniqueness and stability for person identification [1]. A biometric recognition system uses a person's physiological and/or behavioral characteristics as features that include face, fingerprint, palm print, voice patterns, ear, iris and gait. Recently, iris recognition has emerged as a superior method of identification technology. The human iris is an annular region between the pupil (generally darkest portion of the eye) and sclera. It has many interlacing minute characteristics such as freckles, coronas, stripes, furrows, crypts and so on. The iris patterns of the two eyes of an individual or those of identical twins are completely independent and uncorrelated, which is largely determined by the pre-natal development. It is reported that an iris being similar to another oane is of extremely low probability, about 1 in 10^{72} [2]. In addition, the iris is visible, making it highly suitable for practical noninvasive identification processes.

The concept of automated iris recognition is first introduced by Flom and Safir in [2]. Since then, a number of methods have been proposed in the literature for effective iris recognition. In the pioneering work of Daugman [3,4], multiscale Gabor filters are used to demodulate texture phase structure information of the iris. This results in 1024 complex-valued phasors at different scales. Each phasor is quantized to one of the four quadrants in the complex plane. The resulting 2048-component iris code is used to describe an iris. The difference between a pair of iris codes is measured by their Hamming distance. The method of Daugman provides high accuracy and is employed in several commercial iris recognition systems. The drawback of this method is its rather long length of the iris code considering the large volume of iris data to be compared. Wildes [5] represents the iris texture with a Laplacian pyramid constructed with four different resolution levels and uses the normalized correlation to determine whether the input image and the model image are from the same class. However, it gives lower accuracy as compared to that of [3] and suffers from a high computational complexity. Boles and Boashash [6] calculate the zero-crossings of an one-dimensional (1D) wavelet transform at various resolution levels of a concentric circle on an iris image to generate the iris code. In [7], the 4^{th} level Haar wavelet coefficients are quantized to form the iris code, later classified using a competitive learning neural network. In [8], overlapped patches of normalized iris are subjected to discrete cosine transform (DCT); the differences of the coefficients are then quantized to form the iris code, later matched by Hamming distance. In [9], phase components of 2-D Fourier transform coefficients are used as features that are classified using the Hamming distance. In [10], both the phase and magnitude of the Gabor wavelet outputs are used as features that are matched region-wise using the Euclidean distance. In [11], the iris features are extracted using the oriented separable wavelet transforms, called directionlets, and compared using a weighted Hamming distance. In [12], a co-occurrence matrix is generated using the values of various statistical measures calculated from the Contourlet coefficient for matching. In [13], a novel normalization method is employed for iris localization and the corresponding Contourlet coefficients are classified using a Support Vector Machine (SVM). Note that the methods of [12] and [13] report recognition rates for a rather limited number of classes.

Recently, the multi-scale Curvelet transform [14] has emerged as a highly effective tool for sparse image representation, much better than the traditional wavelets. However, to the best of our knowledge very limited work has been done on curvelet transform-based iris recognition

978-1-4673-1154-0/12/$31.00 ©2012 IEEE

[15,16]. In [15], a multimodal biometric recognition system is proposed where the curvelet transform is used to enhance the iris and fingerprint images. The iris features are acquired using gabor filters [4]. In [16], the iris codes are generated from the horizontal and vertical band coefficients by setting those greater than zero to one and the others to zero. The objective of this paper is to introduce an efficient low complexity iris recognition method using the curvelet transform. The performance of the proposed method is studied for various standard databases and compared with that of several existing techniques.

II. IRIS IMAGE DATASETS

The iris data is obtained from three different sources:

(a) CASIA-IrisV3 iris database of National Laboratory of Pattern Recognition, Institute of Automation, Chinese Academy of Sciences [17] and includes three subsets, labeled as CASIA-IrisV3-Interval, CASIA-IrisV3-Lamp, and CASIA-IrisV3-Twins. In total, it contains 22,051 iris images from more than 700 subjects. All iris images are 8 bit gray-level JPEG files, collected under near infrared illumination. Almost all subjects are Chinese except a few in CASIA-IrisV3-Interval. The Interval contains 2639 eye images obtained from 249 subjects with very good quality.

(b) UBIRIS.v1 iris database by SOCIA Lab. – Soft Computing and Image Analysis Group, Department of Computer Science, University of Beira Interior, 6201-001 Covilhã, Portugal [18]; it comprises 1877 images collected from 241 persons in two distinct sessions and incorporating several noise factors. Thus, it enables the evaluation of the robustness of an iris recognition method.

(c) UPOL- Dept. Computer Science, Palacky University, Olomouc [19]; it includes 384 iris images from 64 European persons. The quality of the images is good, without any occlusions by eyelids and eyelashes.

III. CURVELET TRANSFORM

The curvelet transform introduced by Candes and Donoho [14] is an extension of the wavelet concept; however, uses basis functions that are not only localized in location and spatial frequency, but also orientation. The curvelet decomposition can be described in the following steps:

1. Decomposition of the object i.e. image into a sequence of subbands.

2. Windowing of each subband into blocks of appropriate size, depending on its center frequency.

3. Applying the ridgelet transform on those blocks.

By smooth windowing, it is expected that segments of smooth curves would look straight in subimages or (subbands) and thus, can be well captured by a local ridgelet transform. Fig. 1 shows the various basis images for a curvelet transform (CVT) at different scales (i.e. j).

Fig. 2 displays an eye image and its representation in the curvelet transform domain. The low frequency coefficients are located in the approximation subband, at the center of the display. The high frequency coefficients at different scales are represented by the Cartesian concentric coronae where each coronae is divided into four strips. Each strip is subdivided into angular panels where the panel represents a coefficient at a certain scale and orientation, determined by the position of the panel. The sharp localization in both space and frequency is also obvious from Fig. 2.

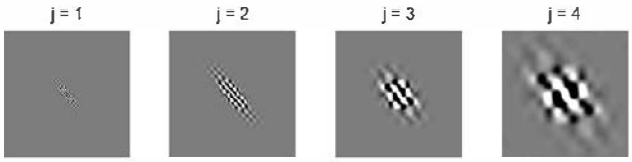

Fig. 1 Basis images from a PDFB that implements the curvelet transform.

Fig. 3 shows the curvelet reconstruction of an eye image. Here, a small percentage (2.5%) of the largest coefficients (in modulus) is selected while the rest set to zero. Next, the inverse curvelet transform is carried out to reconstruct the original image. Note that even with using such small number of coefficients, the image is reconstructed appropriately with the details being preserved.

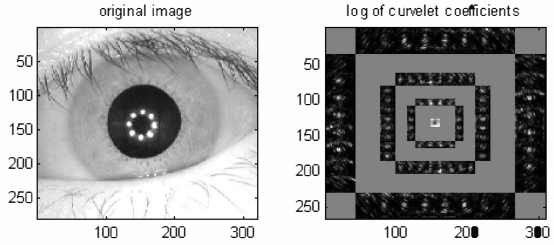

Fig. 2 Curvelet transform of an eye image

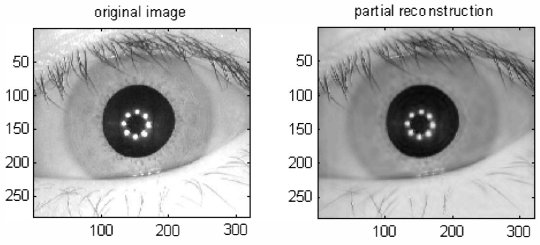

Fig. 3 Partial reconstruction of an eye image using the CVT

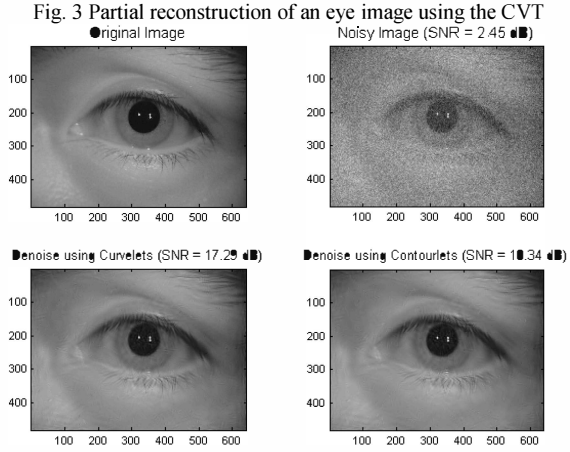

Fig. 4 Denoised images obtained in the CT and CVT domains

Fig. 4 shows the various images obtained by denoising a

noisy eye image in the contourlet and curvelet transform domains. A given eye image is corrupted with additive white Gaussian noise. After transforming the image to contourlet or curvelet domain, all the coefficients except those in the corresponding approximation subband are set to zero. Next, the inverse transform operation is carried out to obtain the denoised image. As seen from Fig. 4, a significant improvement is achieved in terms of signal-to-noise ratio (SNR) and visual quality for the curvelet transform over that of using the contourlet transform. Thus, it indicates a better ability of the curvelet transform to preserve image features as compared to the others even under noise.

IV. PROPOSED IRIS RECOGNITON METHOD

The proposed iris image recognition method consists of three parts: iris localization, feature extraction and matching of the features for image classification. In the preprocessing step, images of irises are extracted from the eye images and normalized to a standard format for feature extraction in order to remove variability introduced by pupil dilation, camera-to-eye distance, head tilt, and torsional eye rotation. All these factors need to be taken into consideration and compensated for in order to generate a final normalized version compliant with the feature extraction input format. The preprocessing is carried out by using the technique of Daugman [3]. The various steps involved in the iris preprocessing are shown in Fig.1. However, the present method does not require the localization of the outer pupil boundary.

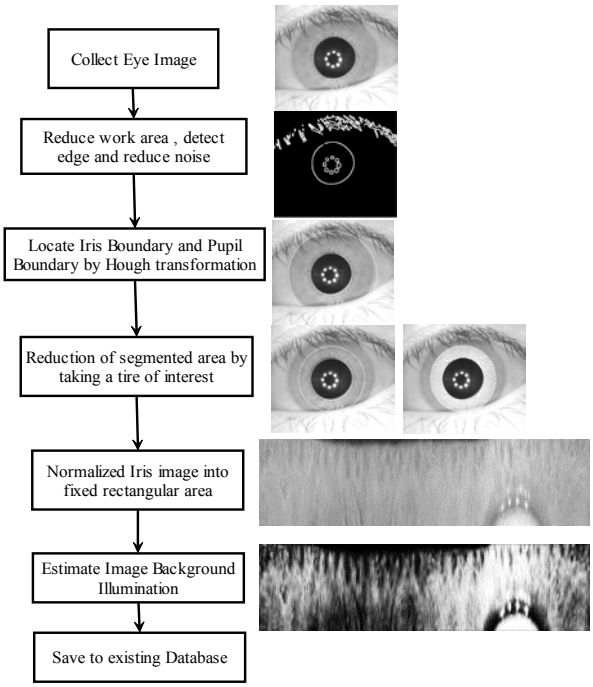

Fig. 5 Steps involved in the generation of an iris image.

Fig. 6 shows the various annular rings surrounding the inner pupil boundary. It is found through extensive experiments that the entropy of a ring becomes almost constant for a width of 31 pixels. Since the entropy of a data represents its information content, in the present paper, instead of using the entire annular patch between the inner pupil and outer pupil boundaries, only the one of width 31 pixels (starting from the inner pupil boundary) is used to generate an iris template image.

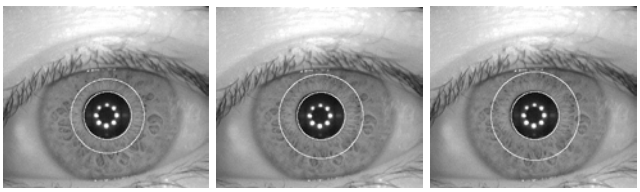

Fig. 6 Annular rings concentric around the inner pupil boundary whose widths are (a) 20, (b) 28 and (c) 31 pixels.

The above-mentioned selection of an area interest concentric around the inner pupil boundary provides several advantages:

(i) Reduction of artifacts such as the eyelash and eyelids since they are almost removed from the image.

(ii) No need to employ any preprocessing technique for the removal of eyelid and eyelash, thus reducing the computational complexity.

(iii) No need localize the outer iris boundary detection, which also reduces the complexity.

(iv) The length of the iris data is decreased that reduces the time required for matching of iris codes since these become smaller in length.

After normalization of the iris image and its enhancement, the corresponding iris features are obtained from its curvelet transform coefficients. The various steps of the process of feature extraction are given below:

1. The Curvelet transformation is applied to a normalized and enhanced iris image.

2. The zero crossings of the 4^{th} level approximation subband coefficients are calculated from their differences.

3. The two dimensional matrix containing the values of the differences are then converted to a one-dimensional vector by taking the row-wise data.

4. The values stored in the vector are binarized by assigning 1 and 0 to positive and negative quantities, respectively. This operation results in a binary code, called iris code that represents the features of the iris image, later used for matching purposes. Fig. 7 shows an iris image along with its retained coefficients and the corresponding iris code.

V. EXPERIMENTAL RESULTS

In the matching process, the correlation coefficient (CC) is used since the iris patterns of the two eyes of an individual or those of identical twins are completely independent and uncorrelated. The matching process is shown in Fig. 8.

The performance of the proposed iris recognition method is compared with the works of Daugman [3], Ma et al. [7], Monro et al. [8], Yingzi Du et al. [10], Vladan [14] and method of [16]. The performance of the various methods is

compared in terms of recognition performance and computation time required during feature extraction and matching.

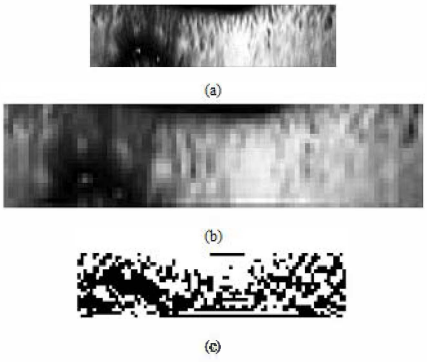

Fig. 7 (a) Iris template image, (b) retained coefficients of the template and (c) corresponding iris code.

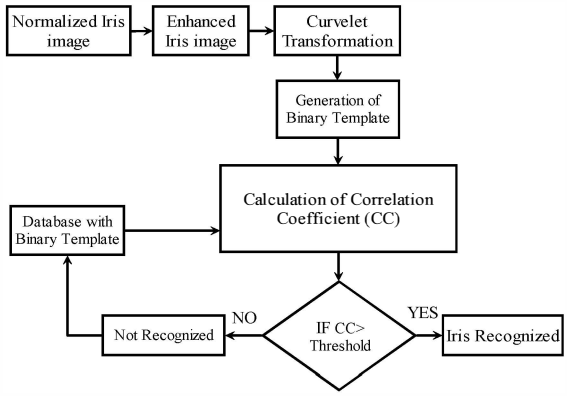

Fig.8 Matching process

VI. EXPERIMENTAL RESULTS

For the curvelet transform, the scaling parameter is set to 0.45. The performance of the proposed method is evaluated using the leave-one-out approach. From each of the databases, CASIA, UPOL and UBIRIS, five images are chosen randomly from each class for matching and testing. Among the five images, one image is used as the test image and others as training images. For identification, the iris code of a test image is matched against the whole database of stored features. The matching resulting in the highest average Correlation coefficient (CC) across the four enrolled images for each class is chosen as the matched iris. The performance of the proposed method is also studied using the CT wherein the coefficients of the approximation subbands of CT are used instead of that of CVT for generating the iris codes. For verification, Receiver Operating Characteristic (ROC) curves are generated by varying a match-cut-off threshold (TH) from 0 to 1 and plotting the False Rejection Rate (FRR) as a function of the False Acceptance Rate (FAR). At a given threshold, the FAR and FRR indicate the probability of accepting an imposter and rejecting a genuine person, respectively. The rate for which FAR becomes equal to FRR is called the equal error rate (EER). The lower the value of EER, the better is the performance of an iris recognition system. The area under the 100% correct recognition is denoted as A-z and calculated from the ROC. Table 1 shows the values of EER, TH and correct recognition rate (CRR) for different databases for the proposed method using both CT and CVT. It can be seen from Table I that the proposed method using CVT provides lower values of EER as compared to that of employing CT, thus indicating a better recognition performance. The Proposed method using the CVT yields higher values of CRR than the CT, more than 97% at the minimum EER for all the databases and almost hundred percent recognition rate for the CASIA database.

TABLE I VALUES OF EER, TH AND CRR FOR DIFFERENT DATABASES

Database	Feature length	Feature Extraction Method	EER	TH	CRR
UBIRIS1	472	CT	0.0314	0.43	0.968
	472	CVT	0.0249	0.41	0.975
CASIA-interval	430	CT	0.01241	0.41	0.989
	430	CVT	0.0112	0.37	0.991
	472	CVT	0.0072	0.41	0.999
	786	WT	0.0138	0.18	0.976
UPOL/Palacky	472	CT	0.0487	0.44	0.972
	472	CVT	0.0447	0.43	0.978

The plots of FRR, FAR and CRR for the proposed method are shown in Fig. 9 for the CASIA V3 database (interval). The value of EER is quite low, of about 0.722% at which the recognition rate is about 99.3%. Also, note that for thresholds below 0.35, the FRR becomes zero, providing a hundred percent correct recognition.

Fig. 10 shows the ROC for the proposed method using CVT, CT, wavelet transform (WT) and discrete cosine transform (DCT). It is seen that among the different ROCs, the area under the one obtained for CVT is smallest with least EER. The values of CRR, A-z and EER obtained for the CASIA V3 (interval) are listed in Table II for the various methods. It is seen that in general, the proposed technique provides higher values of CRR and A-z as compared to those of others. As for the ERR, it gives lower values than that of other methods except the technique of [8]. Table III provides the length of the iris codes for different methods. It is observed that the length of the iris codes for the proposed method is the smallest among the various techniques.

The time required for feature extraction and matching required for the different iris recognition methods are provided in Table IV. It is seen that the proposed method needs the least amount of computational time among the various techniques. The savings in time may be attributed to the modification in preprocessing, use of the coefficients in the approximation subband only and the resulting reduced length of the iris codes.

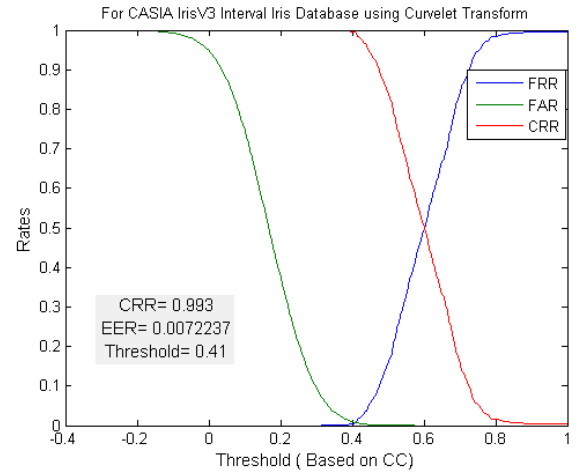

Fig. 9 FAR, FRR and CRR vs. threshold (TH)

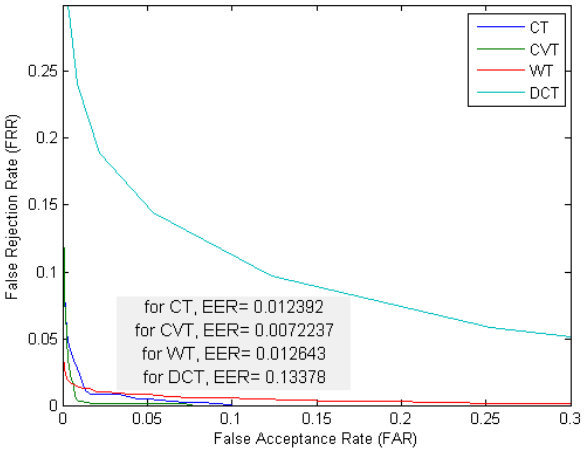

Fig. 10 Plot of ROC for CT, CVT, WT and DCT

TABLE II COMPARISON OF THE PERFORMANCE OF THE VARIOUS METHODS

Method	**CRR (%)**	**A-z**	**EER (%)**
Daugman [3]	91.2	0.978	6.187
Li Ma *et. al.*. [7]	89.7	0.946	7.055
Monro *et. al.* [8]	99	0.99	**0.159**
Vladan [11] n=4 n=8	 90.9 94.3	 0.977 0.987	 5.954 4.321
Yingzi Du *et. al.* [10]	98.1	0.961	1.62
Method of [16]	98	--	--
Proposed method	**99.3**	**1.00**	0.722

TABLE III LENGTH OF IRIS CODES/ FEATURES FOR DIFFERENT METHODS

Method	**Feature Length**
Daugman [3]	2048
Ma *et al.* [7]	10240
Monro *et al.* [8]	3840
Vladan [11] for *n=4* *n=6* *n=8*	 2560 5760 10240
Method of [16]	666
Proposed method	472

TABLE IV COMPARISON BASED ON PROCESSING TIME OF SOME POPULAR IRIS RECOGNITION ALGORITHMS

Method	**Feature Extraction (ms)**	**Match (ms)**	**Feature Extraction and Match (ms)**
Daugman[3]	422	31	453
Ma *et al.* [7]	125	68	193
Monro *et al.* [8]	60	31	91
Vladan[11]	70	1	71
Proposed method	48	6	54

VII. CONCLUSION

In this paper, a low complexity iris recognition method has been proposed based on using the curvelet transform. The zero crossings of the curvelet coefficients have been used to generate the iris codes. It requires the detection of only the inner boundary of the pupil and utilizes a fixed number of pixels from the inner boundary to obtain the iris image. Thus, it reduces the computational time required for iris preprocessing and size of the iris template, hence decreasing the length of the iris code. The matching of a code with another one has been performed by using the correlation coefficient between them. The performance of the proposed method has been studied for several standard databases. It has been shown that the proposed method can provide a very high recognition rate, higher than those of several state-of-the-art techniques while requiring much less computational time.

REFERENCES

[1] Anil K. Jain, Patrick Flynn and Arun A. Ross, "Handbook of biometrics", Springer Science, 2008
[2] Leonard Flom and Aran Safir, "Iris recognition system", U.S. Patent 4 641 349, 1987.
[3] John G. Daugman, "High confidence visual recognition of persons by a test of statistical Independence", IEEE Trans. Pattern Anal. Mach. Intell., vol. 15, no. 11, pp. 1148–1161, 1993.
[4] John G. Daugman, "How iris recognition works", IEEE Trans. Circuits Syst. Video Technol., vol. 14, no. 1, pp. 21–30, 2004.
[5] Ricard P. Wildes, "Iris recognition: an emerging biometrics technology", Proc. IEEE, vol. 85, no. 9, pp. 1348–1363, 1997.
[6] W. Boles and Boualem Boashash, "A human identification technique using images of the iris and wavelet transform", IEEE Trans. Signal Process., vol. 46, pp. 1185–1188, 1998.

[7] Li Ma, Tieniu Tan, Yunhong Wand and Dexin Zhang, "Personal identification based on iris texture analysis", IEEE Trans. Pattern Anal. Mach. Intell., vol. 25, no. 12, pp. 1519–1533, 2003.
[8] Donald M. Monro, Soumyadip Rakshit and D. Zhang, "DCT-based iris recognition," IEEE Trans. Pattern Anal. Mach. Intell., vol. 29, no. 4, pp. 586-595, 2007.
[9] K. Miyazawa, K. Ito, T. Aoki, K. Kobayashi and H., Nakajima, "An effective approach for Iris recognition using phase-based image matching," IEEE Transactions on Pattern Analysis and Machine Intelligence, vol. 30, no. 10, pp. 1741–1756, 2008.
[10] Yingzi Du., Craig Belcher and Zhi Zhou, "Scale invariant gabor descriptor-based noncooperative Iris Recognition", EURASHIP Journal of Advance in Signal Processing, vol. 2010, Article ID 936512, 2010.
[11] Vladan V., "Low-complexity iris coding and recognition based on directionlets," IEEE Transactions on Information Forensics and Security, vol. 4, no. 3, pp. 410–417, 2009.
[12] Amir Azizi and H. Reza Pourreza, "A novel method for iris feature extraction based on contourlet transform and cooccurrence matrix", IADIS International Conference Intelligent Systems and Agents, 2009.
[13] M. Han, W. Sun and M.Li, "Iris recognition based on a novel normalization method and contourlet transform", Proceeding IEEE International Congress on Image and Signal Processing, vol. 1, pp. 1-3, 2009.
[14] Jean-Luc Starck, Emmanual J. Candes and David L. Donoho, "The curvelet transform for image denoising", IEEE Transactions on Image Processing, vol. 11, no. 6, pp. 670—684, 2002.
[15] Adem A. Altun, "Recognition of Selected Fingerprints and Iris Features Enhanced by Curvelet Transform with Artificial Neural Networks", Proceedings of IEEE IWSSIP, pp. 421-424, 2008.
[16] M. Najafi and S. Ghofrani, "Iris recognition based on using ridgelet and curvelet transform", International Journal of Signal Processing, Image Processing and Pattern Recognition, vol. 4, No. 2, June, 2011.
[17] "CASIA-IrisV3", Chinese Academy of Sciences Institute of Automation (CASIA), Beijing, China. [Online].
Available: http://www.cbsr.ia.ac.cn/IrisDatabase.htm
[18] "UBIRIS.v1", Department of Computer Science, University of Beira Interior, 6201-001 Covilhã Portugal.
Available:http://iris.di.ubi.pt/ubiris1.html
[19] http://phoenix.inf.upol.cz/iris/download/